1521-0103/368/1/50–58$35.00
THE JOURNAL OF PHARMACOLOGY AND EXPERIMENTAL THERAPEUTICS

https://doi.org/10.1124/jpet.118.252767
J Pharmacol Exp Ther 368:50–58, January 2019

The Journal of PHARMACOLOGY And Experimental Therapeutics

Prostanoid EP4 Receptor-Mediated Augmentation of I_h Currents in Aβ Dorsal Root Ganglion Neurons Underlies Neuropathic Pain[S]

Hao Zhang, Toshihide Kashihara, Tsutomu Nakada, Satoshi Tanaka, Kumiko Ishida, Satoshi Fuseya, Hiroyuki Kawagishi, Kenkichi Kiyosawa, Mikito Kawamata, and Mitsuhiko Yamada

Departments of Molecular Pharmacology (H.Z., T.K., T.N., H.K., K.K., M.Y.) and Anesthesiology and Resuscitology (H.Z., S.T., K.I., S.F., K.K., M.K.), Shinshu University School of Medicine, Matsumoto, Nagano, Japan

Received August 8, 2018; accepted November 5, 2018

ABSTRACT

An injury of the somatosensory system causes neuropathic pain, which is usually refractory to conventional analgesics, thus warranting the development of novel drugs against this kind of pain. The mechanism of neuropathic pain in rats that had undergone left L5 spinal nerve transection was analyzed. Ten days after surgery, these rats acquired neuropathic pain. The patch-clamp technique was used on the isolated bilateral L5 dorsal root ganglion neurons. The current-clamped neurons on the ipsilateral side exhibited significantly higher excitability than those on the contralateral side. However, only neurons with diameters of 40–50 μm on the ipsilateral side exhibited significantly larger voltage sags in response to hyperpolarizing current pulses than those on the contralateral side. Under the voltage clamp, only these neurons on the ipsilateral side showed a significantly larger density of an inward current at < -80 mV [hyperpolarization-activated nonselective cation (I_h) current] with a rightward-shifted activation curve than that on the contralateral side. Ivabradine—an I_h current inhibitor—inhibited I_h currents in these neurons on both sides in a similar concentration-dependent manner, with an IC_{50} value of ~3 μM. Moreover, the oral administration of ivabradine significantly alleviated the neuropathic pain on the ipsilateral side. An inhibitor of adenylyl cyclase or an antagonist of prostanoid EP4 receptors (CJ-023423) inhibited ipsilateral, but not contralateral I_h, currents in these neurons. Furthermore, the intrathecal administration of CJ-023423 significantly attenuated neuropathic pain on the ipsilateral side. Thus, ivabradine and/or CJ-023423 may be a lead compound for the development of novel therapeutics against neuropathic pain.

Introduction

Neuropathic pain is caused by a lesion or a disease of the somatosensory system (Baron, 2006; Jensen et al., 2011) and is usually refractory to treatment with conventional analgesics (van Hecke et al., 2014). Therefore, the development of novel therapeutics based on the analysis of the pathophysiology of neuropathic pain is highly warranted.

In the somatosensory system, the cell body of the most peripheral neurons is localized in the dorsal root ganglion (DRG) of the spinal nerve (Baron, 2006). DRG neurons are pseudo-unipolar neurons, with an axon splitting into two branches: one branch is oriented toward the periphery and the other toward the spinal cord. DRG neurons are often classified into three subgroups (C, Aδ, and Aα/β) according to their conduction velocity and diameter of the cell body (Harper and Lawson, 1985). Unmyelinated C and myelinated Aδ fibers are small and most frequently transmit nociceptive and thermal information. Myelinated Aα/β fibers are large and mainly committed to transmitting proprioceptive and tactile information. However, approximately one-third of the Aβ neurons are nociceptors (Fang et al., 2005). DRG neurons elicit Na^+ action potentials in response to the activation of their peripheral termini, and in turn activate the secondary sensory neurons on the ipsilateral spinal cord dorsal horn (Baron, 2006).

In neuropathic pain, the peripheral and central somatosensory systems become hypersensitive (Cohen and Mao, 2014). The activities of several ion channels in DRG neurons have been reported to be modified in neuropathic pain (Wickenden et al., 2009). Among them, the hyperpolarization-activated nonselective cation (I_h) currents of the hyperpolarization-activated cyclic nucleotide-gated (HCN) channels are activated and conduct depolarizing inward currents on hyperpolarization after an action potential to induce the next action potential (Foehring and Waters, 1991). The mammalian genome

This study was supported by a grant from Kissei Pharmaceutical Co., Ltd., Matsumoto, Nagano, Japan, awarded to M.Y.; and a Grant-in-Aid for Scientific Research from the Japan Society for the Promotion of Science [Grant 15H02562] awarded to M.K.
https://doi.org/10.1124/jpet.118.252767.
[S] This article has supplemental material available at jpet.aspetjournals.org.

ABBREVIATIONS: COX, cyclooxygenase; DMEM, Dulbecco's modified Eagle's medium; DMSO, dimethylsulfoxide; DRG, dorsal root ganglion; HCN, hyperpolarization-activated cyclic nucleotide-gated; I_h, hyperpolarization-activated nonselective cation; OP, operation; PG, prostaglandin.

contains four genes encoding HCN channel subunits (HCN1–4) (Biel et al., 2009). These subunits form an HCN channel as a tetramer (Lee and MacKinnon, 2017). The cytoplasmic C-terminus of each subunit bears a cyclic nucleotide-binding domain. The cyclic nucleotide-binding domain autoinhibits channel activity, whereas the binding of cAMP to the cyclic nucleotide-binding domain inhibits autoinhibition and activates HCN channels (Wainger et al., 2001). Depending on the extent of autoinhibition, HCN2 and HCN4 are more strongly activated by cAMP than HCN1 or HCN3. In DRGs, Aα/β neurons express mainly HCN1 and also HCN2, whereas C and Aδ neurons express mostly HCN2 and HCN3 (Kouranova et al., 2008; Emery et al., 2011).

An increase in I_h currents may have a causal effect on abnormal nociception—a concept supported pharmacologically (Wickenden et al., 2009) and through the disruption of HCN genes (Momin et al., 2008; Emery et al., 2011). Inflammatory mediators activating adenylate cyclase, such as prostaglandin (PG) E_2 in injured DRGs, have been proposed to induce neuropathic pain by augmenting I_h currents (Emery et al., 2012). However, this finding has not been confirmed, and the type of DRG involved in this process has not been unequivocally identified. Thus, we aimed to clarify these issues in the present study.

Materials and Methods

Ethical Approval. All rats used in this study received humane care in compliance with the Guide for the Care and Use of Laboratory Animals published by the US National Institutes of Health (https://www.ncbi.nlm.nih.gov/books/NBK54050/). All experimental procedures were performed in accordance with the Guidelines for Animal Experimentation of the Shinshu University and were approved by the Committee for Animal Experimentation (Approval No. 280001).

Animals, Chemicals, and Solutions. All adult male Sprague-Dawley rats, weighing 180–220 g, were obtained from Japan SLC Inc. (Hamamatsu, Japan). All rats were provided free access to water and a standard diet throughout the study and were maintained in a controlled room at a temperature of 21–26°C and humidity of 50%–60% under a 12-hour photophase. All efforts were made to minimize animal suffering. Prior to operation (OP) or euthanasia, all rats were deeply anesthetized with 0.3 mg/kg medetomidine, 4.0 mg/kg midazolam, and 5.0 mg/kg butorphanol (intraperitoneally administered) or 3%–3.5% sevoflurane (inhaled).

An adenylyl cyclase inhibitor (SQ22536) was purchased from Abcam (Cambridge, MA). An EP2 receptor antagonist (PF-04418948), hyaluronidase, protease, low-glucose Dulbecco's modified Eagle's medium (DMEM), poly-L-lysine, and laminin were purchased from Merck (Tokyo, Japan). An EP4 receptor antagonist (CJ-023423) and a DP1 receptor antagonist (S-5751) were purchased from Cayman Chemical (Ann Arbor, MI). An IP receptor antagonist (RO1138452) and a PAR2 receptor antagonist (ENMD547) were purchased from Santa Cruz Biotechnology (Heidelberg, Germany). A CGRP receptor antagonist (CGRP; human, 8–37) and a PACAP receptor antagonist (PACAP; human, 6–38) were purchased from Peptide Institute, Inc. (Osaka, Japan). A 5-HT_4 receptor antagonist (GR113808), an HCN channel inhibitor (ivabradine hydrochloride), bovine serum albumin, HBSS(+) with phenol red, and CsCl were purchased from Wako Pure Chemical (Osaka, Japan). Collagenase L was purchased from Nitta Biolab Inc. (Osaka, Japan). DNase I was purchased from Roche (Tokyo, Japan). Insulin, B-27 Minus insulin, and transferrin were purchased from Thermo Fisher Scientific (Waltham, MA). Medetomidine was purchased from Nippon Zenyaku Kogyo Co. (Fukushima, Japan). Midazolam was purchased from Novartis (Tokyo, Japan). Butorphanol was purchased from Meiji Seika Pharma Co. (Tokyo, Japan). Sevoflurane was purchased from Mylan Seiyaku (Osaka, Japan). Borosilicate glass capillaries were purchased from Kimble Glass (Vineland, NJ). Sylgard 184 was purchased from Dow Corning Toray Co. (Tokyo, Japan). The intracellular solution-1 for the measurement of cell membrane potentials contained 140 mM KCl and 1 mM $MgCl_2$ (Wako Pure Chemical); and 0.5 mM EGTA, 3 mM MgATP, and 5 mM HEPES (Dojindo, Kumamoto, Japan) (pH 7.3 with KOH; Wako Pure Chemical). The extracellular bath solution-1 for the measurement of cell membrane potentials contained 136.5 mM NaCl, 5.4 mM KCl, 1.8 mM $CaCl_2$, 0.53 mM $MgCl_2$, 5.5 mM HEPES, and 5.5 mM glucose (pH 7.4 with NaOH; all from Wako Pure Chemical). The intracellular solution-2 for the measurement of I_h currents contained 130 mM D-aspartate, 10 mM NaCl, 0.5 mM $MgCl_2$, 1 mM EGTA, 5 mM HEPES, and 2 mM MgATP (pH 7.2 with KOH). The extracellular bath solution-2 for the measurement of I_h currents contained 136.5 mM NaCl, 5.4 mM KCl, 1.8 mM $CaCl_2$, 0.53 mM $MgCl_2$, 5.5 mM HEPES, 5.5 mM glucose, 1 mM $BaCl_2$, 0.1 mM $NiCl_2$, 0.1 mM $CdCl_2$, and 0.01 mM nifedipine (pH 7.4 with NaOH; all from Wako Pure Chemical).

Neuropathic Pain Models. To transect the L5 spinal nerve, the rats were anesthetized with 3%–3.5% sevoflurane in 100% oxygen and placed in the prone position to shave their lower back areas. Thereafter, a 2-cm-long incision was made at the level of the posterior iliac crest to access the lumbar spinal nerves. The bilateral L4, L5, and L6 spinal nerves were dissected carefully. Subsequently, only the left L5 spinal nerve was firmly double-ligated with 6-0 silk suture and transected at the center between the two ligations (LaBuda and Little, 2005; Jaggi et al., 2011). These surgical procedures did not alter the size distribution of DRG neurons significantly, except for a significant decrease in the number of neurons with diameters of 50–60 μm on the ipsilateral side (Supplemental Fig. 1). The pathophysiological significance of this observation was not clarified in the present study. These surgical procedures induced established neuropathic pain on the ipsilateral hind paw of the rat by the 10th day after OP (Figs. 4B and 6).

Assessment of Tactile and Thermal Sensitivity. Ten days after OP, the tactile and thermal sensations of rats were assessed as follows: the von Frey test was used to detect the mechanical threshold in the hind paw region. Calibrated von Frey filaments (Danmic Global, LLC, San Jose, CA) were used to measure mechanical nociception. The rats were placed in a transparent poly(methyl methacrylate) box. Calibrated von Frey filaments were applied to the hind paw of unrestrained rats to test the mechanical response. A series of 10 von Frey filaments (10, 14, 20, 40, 60, 80, 100, 150, 260, and 600 mN forces) were used. Each filament was applied perpendicularly to the plantar surfaces of the bilateral hind paws with sufficient force to bend the filaments five times at intervals of 6 seconds. We determined the 50% mechanical withdrawal threshold using the "up-down method" described elsewhere (Chaplan et al., 1994). Paw withdrawal latency to noxious heat stimuli was assessed by applying a focused radiant heat source (model 37370; Ugo Basil, Comerio, Italy) to the bilateral hind paws of unrestrained rats. Brisk withdrawal or licking of the paw following the stimulus was considered as a positive response. To avoid tissue damage to the paws, a cutoff period of 20 seconds was imposed.

In Vivo Drug Administration. To assess the effect of an I_h current inhibitor—ivabradine—on neuropathic pain after spinal nerve injury, 1 ml of saline or the drug dissolved in 1 ml saline (6 mg/kg) was administered twice a day for 4 days from the 10th day after OP. Saline or ivabradine was administered orally through a gastric sonde over a period of 10–15 seconds, 3 hour prior to, and 3 hours after assessment of tactile and thermal sensitivity. The tube was inserted gently from the mouth to the stomach.

To assess the effect of an EP4 receptor antagonist, CJ-023423, on neuropathic pain after spinal nerve injury, intrathecal catheterization was performed under anesthesia with 3%–3.5% sevoflurane on the fifth day after OP (Yaksh and Rudy, 1976). A polyethylene-10 catheter was inserted through an incision in the atlanto-occipital membrane.

The catheter was advanced in the caudal direction by 8 cm from the incision site to the lumbar enlargement of the spinal cord. The external end of the catheter was tunneled subcutaneously to exit at the top of the head and plugged with a piece of steel wire. The skin was closed using 3-0 silk suture. The catheterized rats were kept in individual cages and allowed to recover for <5 days. Rats exhibiting normal behavior and weight gain were used for further experiments. To examine the effect of intrathecal administration of the EP4 receptor antagonist CJ-023423, it was first dissolved in 100% dimethylsulfoxide (DMSO) at 300 mM and then diluted 1000 times with saline (to achieve final concentrations of 300 μM CJ-023423 and 0.1% DMSO). Subsequently, 10 μl of the solution containing 300 μM CJ-023423 plus 0.1% DMSO or only 0.1% DMSO was administered to the rats intrathecally, followed by an injection of 10 μl of saline to flash out the solutions remaining in the catheter. Their effects on the contralateral and ipsilateral sensations were assessed with the aforementioned method before and 10–60 minutes after the injection. The drugs or vehicles were assigned randomly to rats to avoid potential bias.

Isolation of DRG Neurons. Ten to 13 days after the OP, the rats were anesthetized with 0.3 mg/kg medetomidine, 4 mg/kg midazolam, and 5 mg/kg butorphanol (intraperitoneally administered) and sacrificed. Bilateral L5 DRGs were excised from the animals, transferred to Ca^{2+}-free Tyrode solution, minced with fine scissors, and digested with 1 mg/ml collagenase, 0.07 mg/ml protease, 0.5 mg/ml bovine serum albumin, 1.25 mg/ml hyaluronidase, and 0.01 mg/ml DNase I for 55 minutes. This digestion was terminated with a solution of 9.35 ml DMEM, 0.25 ml insulin, 0.2 ml B-27 Minus insulin, and 1 mg transferrin. Subsequently, the cell suspension was centrifuged at 500 rpm for 8 minutes, and the supernatant was discarded. The cell pellet was resuspended in 50 μl DMEM supplemented with 10% fetal bovine serum, 100 U/ml penicillin, and 100 μg/ml streptomycin. Then, 15 μl of the cell suspension was transferred onto a 0.02% poly-L-lysine- and 0.1 mg/ml laminin-coated 15-mm coverslip in a 35-mm dish. After 90 minutes, 2 ml DMEM was added to the 35-mm dish, and the dish was stored at 37°C and 5% CO_2 until further use.

Electrophysiological Analyses. After 2–4 hours of isolation of the DRG neurons, the cells on the coverslip were transferred to an organ chamber on the stage of an inverted microscope. Then, the membrane potentials and currents of the DRG neurons were measured in the whole-cell configuration of the patch-clamp technique with a patch-clamp amplifier (Axopatch 200B; Molecular Devices, Sunnyvale, CA). The membrane potential and channel currents were recorded at room temperature and digitized at 5 kHz after being low-pass filtered at 2 kHz (Kashihara et al., 2017). Patch pipettes (3 to 4 MΩ) were fabricated from borosilicate glass capillaries and coated with Sylgard 184. Series resistance was always kept at <7 MΩ and routinely compensated using the amplifier by ~75%. DRG neurons were divided into four groups according to the diameter of their cell body: Φ = 20–30, 30–40, 40–50, and 50–60 μm, as measured using an ocular micrometer in an inverted microscope. The membrane potentials were recorded using the intracellular solution-1 and extracellular bath solution-1 under the current-clamp condition. Rectangular depolarizing or hyperpolarizing current pulses with different amplitudes were applied to cells for 1000 milliseconds to measure the rheobase or voltage sag, respectively. The I_h currents were recorded using the intracellular solution-2 and extracellular bath solution-2 under the voltage-clamp condition. The membrane potential was hyperpolarized from the holding potential (−40 mV) to potentials of −50 to −130 mV for 4500 milliseconds with a 10-mV decrement (P1), followed by a pulse to −100 mV for 500 milliseconds (P2) every 10 seconds. The I_h currents were isolated as the current inhibited by CsCl (5 mM) in the external bath solution. The amplitude of the I_h currents was normalized to the cell membrane capacitance measured with the amplifier to assess the I_h current density (p*A*/p*F*). The amplitude of peak tail currents in P2 was measured, normalized to the maximum, plotted against the potential at P1, and fitted with the following Boltzmann function to evaluate the activation curve of I_h currents:

$$d = 1/\{1 + \exp[(E_{1/2} - E_m)/k]\} \quad (1)$$

where d is the activation; $E_{1/2}$ is the half-maximum activation potential; E_m is the membrane potential; and k is the slope factor of activation. The activation kinetics of I_h currents in P1 were estimated by fitting the channel current density at different membrane potentials with the following double-exponential function:

$$I = A_0 + A_f \exp(-t/t_f) + A_s \exp(-t/\tau_s) \quad (2)$$

where I is the I_h current density; A_0 is the amplitude of the steady-state I_h current density; A_f and A_s are the amplitudes of the fast and slow components, respectively; t is the time after the initiation of P1;

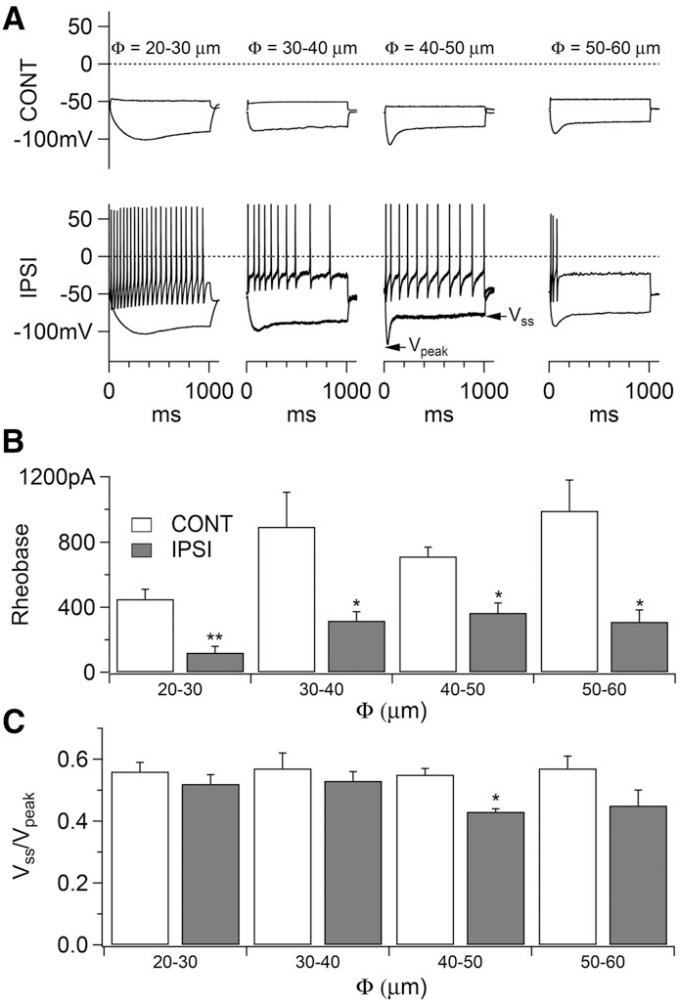

Fig. 1. Membrane excitability of DRG neurons after spinal nerve injury. (A) Representative responses of DRG neurons of different sizes on the contralateral side (CONT) and ipsilateral side (IPSI) to hyperpolarizing and depolarizing currents under the current-clamp condition. The amplitudes of hyperpolarizing and depolarizing currents were +100 and −200, +150 and −700, +400 and −500, and +500 and −700 pA for DRG neurons with diameters of 20–30, 30–40, 40–50, and 50–60 μm, respectively. (B) The rheobase of DRG neurons of different sizes on the contralateral and ipsilateral sides; N = 5 to 6 for each group. (C) The ratio of the steady-state to the peak membrane potential (V_{ss}/V_{peak}) of DRG neurons of different sizes on the contralateral and ipsilateral sides in response to hyperpolarizing current pulses; N = 5 to 6 for each group. The method of measurement for the V_{peak} and V_{ss} is illustrated in (A). Significant difference is indicated as follows: *$P < 0.05$; **$P < 0.01$ vs. the contralateral side.

and τ_f and τ_s are the time constants of the fast and slow components, respectively.

When the effect of pharmacological inhibitors on I_h currents was assessed, DRG neurons were pretreated with different concentrations of drugs for 30 minutes prior to the measurement of the current density/voltage relationships of I_h currents. To estimate the concentration-response relationship of the effect of ivabradine on I_h currents at −100 mV, the effect of different concentrations of ivabradine on the amplitude of the normalized steady-state I_h current density was plotted against the concentration of the agent and fitted with the following Hill equation:

$$I = 1/\left[1 + \left([\text{Iva}]/K_{1/2}\right)^n\right] \quad (3)$$

where I is the normalized amplitude of the steady-state I_h current density at −100 mV; [Iva] is the concentration of ivabradine; $K_{1/2}$ is the half-maximum inhibitory concentration of ivabradine; and n is the Hill coefficient.

Statistical Analysis. The data are shown as the mean ± S.E.M. Student's unpaired t test was used to evaluate the statistical significance. The significant difference is indicated as follows: $^*P < 0.05$, $^{**}P < 0.01$, and $^{***}P < 0.001$.

Results

Increased Excitability of DRG Neurons after Spinal Nerve Injury. Bilateral L5 DRG neurons, in which neuropathic pain had been established in the rats, were enzymatically isolated 10–13 days after left spinal nerve injury. Under the current-clamp condition, depolarizing and hyperpolarizing currents were applied to the neurons. All sizes of neurons on the ipsilateral side exhibited stronger excitability in response to depolarizing currents than those on the contralateral side (Fig. 1A; Table 1). Figure 1B summarizes the rheobase of these cells (N = 5 to 6 for each group). Neurons on the ipsilateral side showed significantly lower rheobase than that observed on the contralateral side, regardless of the cell size. This hyperexcitability after nerve injury is known to occur due to the remodeling of various ion channels, such as voltage-dependent Na^+, Ca^{2+}, and K^+ channels; transient receptor potential channels; and HCN channels (Wickenden et al., 2009; Krames, 2014). A voltage sag in response to a hyperpolarizing current pulse is indicative of HCN channel currents (I_h currents). The voltage sag was more evident in neurons with diameters of 40–50 and 50–60 μm than in smaller neurons (Fig. 1A). Notably, the voltage sag was increased significantly after nerve injury only in neurons with diameters of 40–50 μm on the ipsilateral side (N = 5 to 6 for each group) (Fig. 1C). These results indicate that an increase in I_h currents may account for the hyperexcitability of neurons with diameters of 40–50 μm, whereas that of the other neurons probably depends on other mechanisms.

Altered I_h Current Density/Voltage Relationship after Spinal Nerve Injury. Figure 2A shows the representative I_h current density in response to rectangular hyperpolarizing voltage steps between −50 and −130 mV in a 10-mV decrement from the holding potential of −40 mV. On the contralateral side, the amplitude of the I_h current density was proportional to the size of the neurons (Scroggs et al., 1994). On the ipsilateral side, neurons with diameters of

TABLE 1
Cell membrane characteristics of DRG neurons under the current-clamp condition
Significant difference is indicated as follows: $^*P < 0.05$; $^{**}P < 0.01$; $^{***}P < 0.001$.

Cell Diameter	Contralateral	Ipsilateral	Significant Difference
μm			
V_{rest} (mV)			
Φ = 20–30	−57.78 ± 0.96	−53.15 ± 1.39	*
Φ = 30–40	−57.68 ± 2.79	−55.33 ± 2.12	NS
Φ = 40–50	−59.02 ± 1.52	−54.14 ± 2.06	NS
Φ = 50–60	−60.84 ± 0.98	−50.60 ± 0.93	***
Rheobase (nA)			
Φ = 20–30	0.45 ± 0.06	0.12 ± 0.04	**
Φ = 30–40	0.90 ± 0.21	0.32 ± 0.06	*
Φ = 40–50	0.71 ± 0.06	0.37 ± 0.06	*
Φ = 50–60	0.99 ± 0.19	0.31 ± 0.07	*
V_{ss}/V_{peak}			
Φ = 20–30	0.56 ± 0.03	0.52 ± 0.03	NS
Φ = 30–40	0.57 ± 0.05	0.53 ± 0.03	NS
Φ = 40–50	0.55 ± 0.02	0.43 ± 0.01	**
Φ = 50–60	0.57 ± 0.04	0.45 ± 0.05	NS

NS, not significantly different; V_{rest}, resting membrane potential; V_{ss}/V_{peak}, ratio of the steady-state membrane potential to the peak membrane potential elicited by hyperpolarizing current injection.

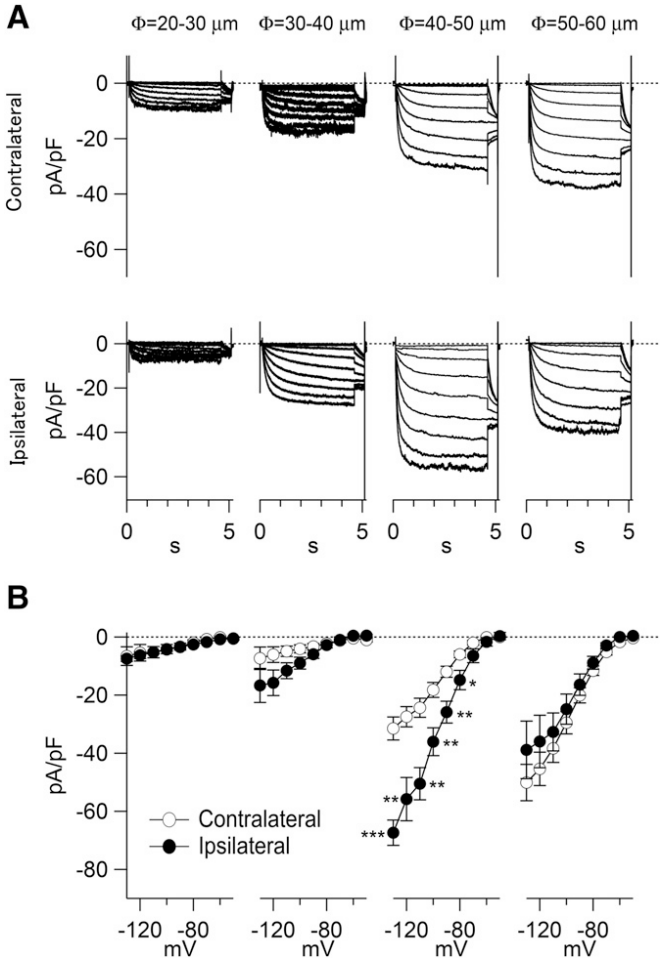

Fig. 2. Steady-state I_h current density/voltage relationship of DRG neurons after spinal nerve injury. (A) Representative I_h current density of DRG neurons of different sizes on the contralateral and ipsilateral sides in response to rectangular hyperpolarizing voltage steps between −50 and −130 mV in a 10-mV decrement from the holding potential of −40 mV. (B) The summary of the steady-state I_h current density/voltage relationship of DRG neurons of different sizes on the contralateral and ipsilateral sides. N = 6–9 for each group. The significant difference is indicated as follows: $^*P < 0.05$; $^{**}P < 0.01$; $^{***}P < 0.001$ vs. the contralateral side.

40–50 μm showed larger amplitudes of the I_h current density, whereas the rest of the neurons showed comparable amplitudes of the I_h current density with those reported on the contralateral side. Figure 2B summarizes the steady-state I_h current density/voltage relationship (N = 6–9 for each group). Only neurons with diameters of 40–50 μm on the ipsilateral side exhibited significantly and as much as two times larger I_h current density at < -80 mV than those observed on the contralateral side.

Kinetic Analysis of I_h Currents after Spinal Nerve Injury. Figure 3A explains the analysis method for the kinetics of I_h currents. An arrow indicates the peak tail current density at -100 mV measured to calculate the activation curve of I_h currents (Fig. 3B). Figure 3B depicts the relationship between the membrane potential and activation (symbols and bars) and its fit with the Boltzmann function (lines) (N = 5–7 for each group) (eq. 1). Only neurons with diameters of 40–50 μm on the ipsilateral side showed a significant depolarization shift of their activation curve compared with those on the contralateral side (Table 2). In addition, Fig. 3A illustrates the representative fitting of the I_h current density at different membrane potentials with biexponential function (black lines) (eq. 2). Figure 3C summarizes the fast and slow time constants (τ_f and τ_s) and the fraction of the fast and slow components (A_f and A_s) (N = 5–7 for each group). In these neurons, on both sides, τ_f and τ_s decreased, whereas A_f predominated A_s when the membrane potential was hyperpolarized. However, this tendency was not necessarily clear in neurons with diameters of 20–30 μm because their I_h current density was extremely small to reliably fit into eq. 2 in most cases. No significant difference was detected in these parameters between the contralateral and ipsilateral sides, irrespective of the cell size. These results indicate that only neurons with diameters of 40–50 μm on the ipsilateral side showed a significant increase in the amplitude of the I_h current density as well as a significant depolarizing shift of their activation curve compared with those on the contralateral side.

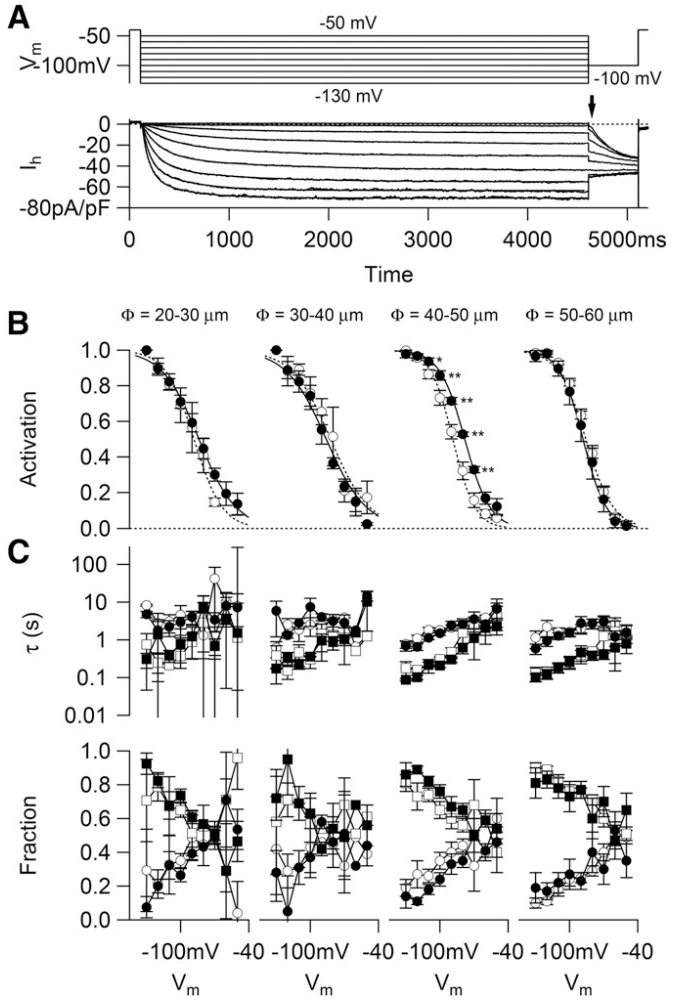

Fig. 3. Kinetics of the I_h current density of DRG neurons after spinal nerve injury. (A) Representative double-exponential fitting of the I_h current density (continuous black lines) and the peak tail current density at -100 mV (arrow) measured to calculate the activation curve of I_h currents. (B) The activation curve of I_h currents of DRG neurons of different sizes on the contralateral and ipsilateral sides was plotted against the membrane potential (symbols and bars) and fitted with a Boltzmann function (lines); N = 5–7 for each group (eq. 1). (C) The voltage dependency of parameters used for the double-exponential fitting of I_h currents (eq. 2); N = 5–7 for each group. In the graphs in the upper row, contralateral τ_s (○), contralateral τ_f (□), ipsilateral τ_s (●), and ipsilateral τ_f (■) are shown. In the graphs in the lower row, contralateral A_s (○), contralateral A_f (□), ipsilateral A_s (●), and ipsilateral A_f (■) are shown. Significant difference is indicated as follows: $^*P < 0.05$; $^{**}P < 0.01$ vs. the contralateral side.

Ivabradine Decreases the Amplitude of I_h Current Density in a Concentration-Dependent Manner and Significantly Inhibits Neuropathic Pain after Spinal Nerve Injury. Hence, we focused on I_h currents in neurons with diameters of 40–50 μm and their pathophysiological significance in neuropathic pain. Ivabradine is a nonselective HCN channel inhibitor, inhibiting neuronal I_h currents and cardiac I_f currents (Bucchi et al., 2006; Wickenden et al., 2009). In this study, ivabradine inhibited I_h currents in neurons with diameters of 40–50 μm on both sides in a similar concentration-dependent manner with a $K_{1/2}$ value of ~2.5 μM and a Hill coefficient (n) of ~1 (eq. 3) (N = 14 for each group) (Fig. 4A). Figure 4B shows that spinal nerve injury induced the ipsilateral mechanical and thermal hypersensitivities by the 10th day after OP. The oral administration of 12 mg/kg per day of ivabradine twice a day for 4 days from the 10th day after OP significantly alleviated the hypersensitivity on the ipsilateral side (N = 5–7 for each group), as reported earlier (Descoeur et al., 2011; Noh et al., 2014; Young et al., 2014). These results indicate that the increased I_h current density in neurons with diameters of 40–50 μm has a causal effect on

TABLE 2
Activation parameters of I_h channels for different sizes of DRG neurons
Significant difference is indicated as $^{**}P < 0.01$.

Cell Diameter	Contralateral	Ipsilateral	Significant Difference
μm			
$E_{1/2}$ (mV)			
Φ = 20–30	−85.45 ± 2.85	−81.45 ± 1.72	NS
Φ = 30–40	−79.80 ± 7.95	−85.85 ± 0.45	NS
Φ = 40–50	−89.72 ± 2.51	−76.64 ± 2.54	**
Φ = 50–60	−85.86 ± 1.58	−88.03 ± 4.24	NS
k (mV)			
Φ = 20–30	7.12 ± 3.09	17.36 ± 4.45	NS
Φ = 30–40	15.67 ± 1.47	17.65 ± 4.45	NS
Φ = 40–50	15.60 ± 1.62	13.83 ± 1.86	NS
Φ = 50–60	11.93 ± 0.41	10.29 ± 1.08	NS

$E_{1/2}$, half-maximum activation potential of I_h channels; k, slope factor of the activation curve of I_h channels; NS, not significantly different.

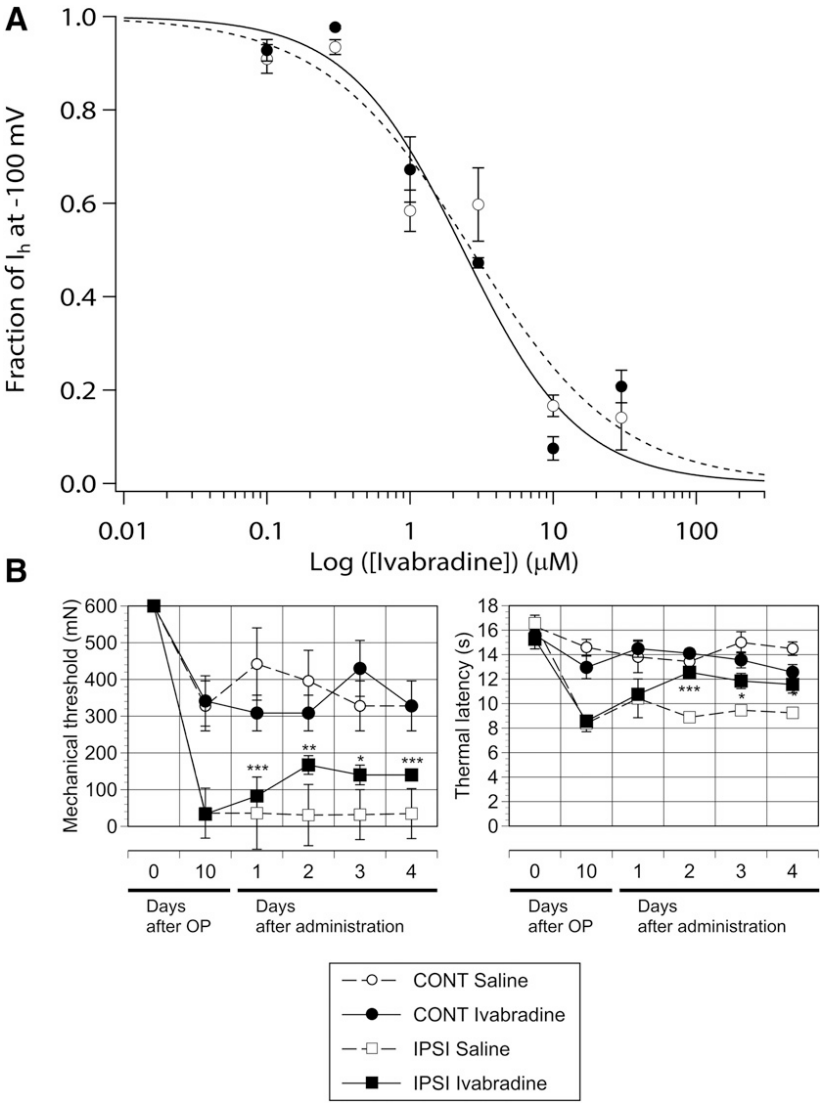

Fig. 4. The effect of ivabradine on I_h currents of DRG neurons and neuropathic pain. (A) The concentration-dependent inhibition of the I_h current density at −100 mV of DRG neurons with diameters of 40–50 μm on the contralateral and ipsilateral sides; $N = 14$ for each group. In the graphs, the contralateral effect of ivabradine (○) and the ipsilateral effect of ivabradine (●) are shown. Curves represent the fitting of the concentration-response relationship with the Hill equation (eq. 3). (B) The effect of the oral administration of 12 mg/kg per day of ivabradine on the mechanical and thermal hypersensitivities after spinal nerve injury. Ivabradine was administered daily to rats for 4 days from the 10th day after the OP; $N = 5$–7 for each group. The In graphs, contralateral saline (○), contralateral ivabradine (●), ipsilateral saline (□), and ipsilateral ivabradine (■) are shown. Significant difference is indicated as follows: $^*P < 0.05$; $^{**}P < 0.01$; $^{***}P < 0.001$ vs. saline on the same side.

neuropathic pain and that ivabradine may be used to treat neuropathic pain.

Mechanism of Increase in I_h Currents after Spinal Nerve Injury. Finally, we analyzed the mechanism of increase in the I_h current density after spinal nerve injury. It has been established that the I_h current density in DRG neurons is increased by cytosolic cAMP (Wickenden et al., 2009). In the present study, the adenylate cyclase inhibitor SQ22536 (1 mM) significantly inhibited the increase in I_h currents in ipsilateral neurons with diameters of 40–50 μm ($N = 5$ to 6 for each group) (Fig. 5) (Emery et al., 2013). Adenylate cyclase is activated by G_s-protein-coupled receptors. In DRG neurons, G-protein-coupled receptors, such as PAR2, DP1, IP, EP2, EP4, CGRP, PACAP, and 5-HT_4 receptors, have been shown to couple with G_s (Jongsma et al., 2000; Segond von Banchet et al., 2002; Ossovskaya and Bunnett, 2004; Moriyama et al., 2005; Ebersberger et al., 2011; Godínez-Chaparro et al., 2012; Yokoyama et al., 2013; Ma and St-Jacques, 2018). Among their antagonists, only the EP4 receptor antagonist CJ-023423 (3 μM) significantly inhibited the increase in I_h current in ipsilateral neurons with diameters of 40–50 μm ($N = 5$–7 for each group) (Fig. 5) (Jones et al., 2009). Figure 6 shows that the intrathecal administration of CJ-023423 acutely and significantly ameliorated neuropathic pain on the 10th day after spinal nerve injury ($N = 5$ for each group). These results indicate that PGE_2-stimulated EP4 receptors probably increase the I_h current density in ipsilateral neurons with diameters of 40–50 μm through cAMP, thereby causing neuropathic pain. In addition, these results indicate that CJ-023423 may be useful to treat neuropathic pain.

Discussion

In this study, we found that left L5 spinal nerve injury in rats resulted in neuropathic pain, and a significant increase in the I_h current density with a rightward shift of the activation curve in ipsilateral DRG neurons with diameters of 40–50 μm compared with those observed on the contralateral side. This increase was mediated by EP4 receptor-stimulated adenylyl cyclase. It is possible that increased cytosolic cAMP activated the HCN2 channels in these neurons. Moreover, the suppression of the increased I_h current density either directly using the I_h current inhibitor ivabradine, or indirectly using the EP4-receptor antagonist CJ-023423, significantly attenuated the mechanical and thermal hypersensitivities on the ipsilateral side of the hind paws of rats. DRG neurons of this size are

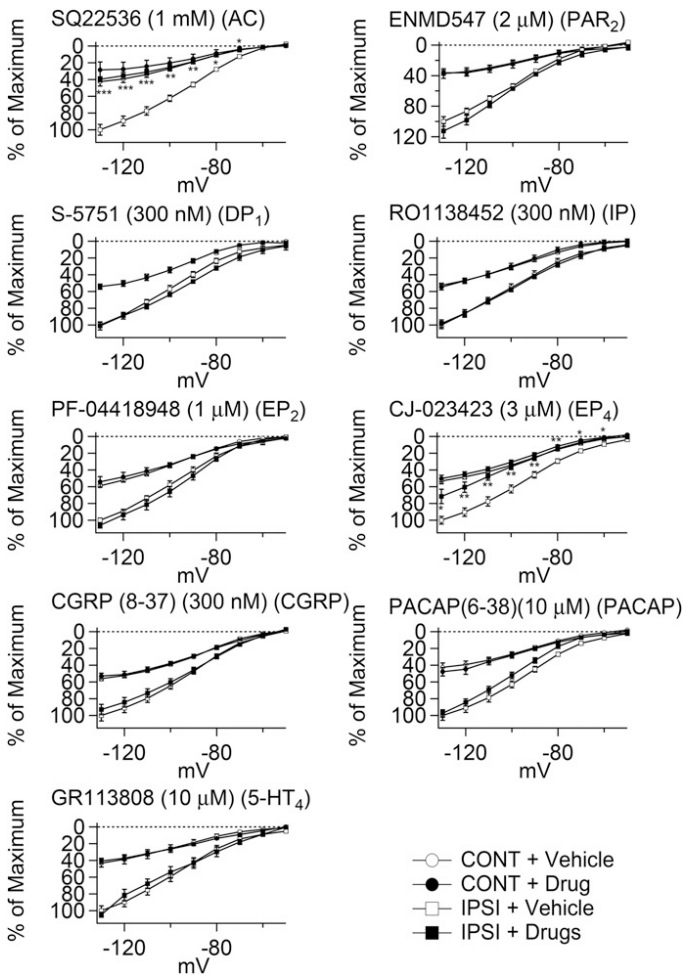

Fig. 5. The effect of inhibition of adenylyl cyclase on I_h currents of DRG neurons and neuropathic pain. Effect of DMSO, SQ22536 (1 mM) (adenylyl cyclase inhibitor), ENMD547 (2 μM) (PAR2 receptor antagonist), S-5751 (300 nM) (DP1 receptor antagonist), RO1138452 (300 nM) (IP receptor antagonist), PF-04418948 (1 μM) (EP2 receptor antagonist), CJ-023423 (3 μM) (EP4 receptor antagonist), CGRP(8–37) (300 nM) (CGRP receptor antagonist), PACAP(6–38) (10 μM) (PACAP receptor antagonist), and GR113808 (10 μM) (5-HT_4 receptor antagonist) on the steady-state I_h current density/voltage relationships of DRG neurons with diameters of 40–50 μm on the contralateral and ipsilateral sides; N = 5–7 for each group.

classified as Aα/β neurons. Among them, Aα neurons are pure proprioceptors, and most of the Aβ neurons are sensors of tactile information, whereas one-third of the Aβ neurons are nociceptors. Thus, it is possible that the PGE_2-mediated augmentation of the I_h current density in nociceptive Aβ neurons has a causal effect on neuropathic pain.

We found that all DRG neurons on the ipsilateral side, irrespective of their size, showed significantly lower rheobase than those on the contralateral side (Fig. 1B). This finding indicates that these neurons exhibited enhanced excitability; thus, all of them may contribute to neuropathic pain. However, we found that only ipsilateral neurons with diameters of 40–50 μm exhibited a significantly larger voltage sag in response to hyperpolarizing current pulses than those on the contralateral side (Fig. 1C). Consistent with this finding, the voltage-clamp experiments revealed that only these neurons had a significantly larger I_h current density with a rightward shift of their activation curve than those on the contralateral side (Fig. 2). Therefore, it is possible that these ipsilateral neurons became hyperactive due to the increased I_h current density, whereas other ipsilateral DRG neurons became hyperactive because of the changes in other ion channels (Wickenden et al., 2009; Krames, 2015). This may, in part, account for ivabradine or CJ-023423 significantly alleviating, but not abolishing, neuropathic pain completely (Fig. 4B; Fig. 6).

Ipsilateral Aβ DRG neurons exhibited a rightward shift of the activation curve (Fig. 3B), which is indicative of the cAMP-mediated regulation of the HCN2 and HCN4 channels (Biel, 2009). Since HCN4 exhibited low levels of expression in DRG neurons even under a neuropathic condition (Wickenden et al., 2009), it is possible that the HCN2 channels are responsible for this change. The I_h currents in neurons of this size have been shown to be mediated by the HCN1 and HCN2 channels (Kouranova et al., 2008; Momin et al., 2008; Emery et al., 2011). We could not confirm the possibility that HCN2 transcripts were increased in these ipsilateral neurons, as assessed with single-cell quantitative real-time polymerase chain reaction (data not shown). This finding is consistent with the fact that the inhibition of adenylate cyclase almost completely normalized the I_h currents in these neurons (Fig. 5). Thus, the augmentation of I_h currents was possible due to the cAMP-dependent activation of the HCN2 channels. In that case, a puzzling finding was the lack of significant changes in the parameters describing the time course of the activation of I_h currents (i.e., τ_f, τ_s, A_f, or A_s) in these neurons. It was established that the HCN2 channels have slower activation kinetics than HCN1 channels and that cAMP accelerates the activation kinetics of HCN2 channels (Wickenden et al., 2009). We, therefore, hypothesize that the activation of I_h currents in ipsilateral DRG neurons with diameters of 40–50 μm was not apparently accelerated compared with those on the contralateral ones because the former have large and fast HCN1 currents and enlarged and accelerated HCN2 currents, while the latter have large and fast HCN1 currents and small and slow HCN2 currents. In this case, the effect of cAMP on the I_h current kinetics may be obscure, not reaching statistical significance.

We found that the nonselective HCN channel inhibitor ivabradine was almost equipotent in inhibiting I_h currents in these DRG neurons on both sides (Fig. 4A). To the best of our knowledge, this is the first study to show that ivabradine is as equipotently effective in inhibiting the ipsilateral augmented I_h currents as contralateral normal I_h currents (Descoeur et al., 2011; Noh et al., 2014; Young et al., 2014). In addition, the prolonged oral administration of ivabradine significantly alleviated the mechanical and thermal hypersensitivities on the ipsilateral side. It would thus be reasonable to consider that under in vivo conditions, ivabradine also inhibited I_h currents in the other neurons. However, the drug did not affect nociceptive sensitivity on the contralateral side (Fig. 4B), which indicates that I_h currents are not involved in normal nociception.

We found that the EP4 receptor-mediated activation of adenylate cyclase resulted in the remodeling of I_h currents in ipsilateral Aβ neurons (Fig. 5). This observation is consistent with that of a previous report showing that knockout of adenylate cyclase 5, a membrane-associated PGE synthetase-1, or HCN2 inhibited neuropathic pain after nerve injury (Mabuchi et al., 2004; Kim et al., 2007; Emery et al., 2011). In the present study, the EP4 receptor antagonist CJ-023423 was effective both in vivo and in vitro after the enzymatic isolation

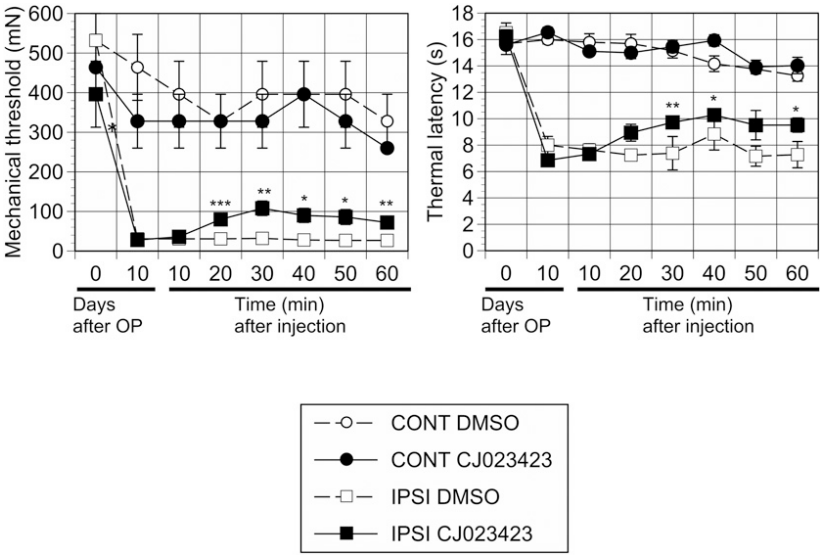

Fig. 6. The effect of the intrathecal administration of CJ-023423 (EP4 receptor antagonist) on the mechanical and thermal hypersensitivities after spinal nerve injury. CJ-023423 (300 μM $\times$ 10 μl) or DMSO (0.1% $\times$ 10 μl) was administrated intrathecally to rats on the 10th day after the OP; $N = 5$ for each group. In the graphs, contralateral vehicle (○), contralateral drug (●), ipsilateral vehicle (□), and ipsilateral drug (■) are shown. Significant difference is indicated as follows: $^*P < 0.05$; $^{**}P < 0.01$; $^{***}P < 0.001$ vs. vehicle on the same side.

of DRG neurons (Fig. 5). Thus, it is most likely that these ipsilateral neurons autocrined PGE_2 or overexpressed EP4 receptors. However, we did not detect increased expression of cyclooxygenase (COX) 1, COX2, or EP4 receptors in neurons with different sizes on the ipsilateral versus the contralateral side, as assessed with single-cell quantitative real-time polymerase chain reaction or western blotting (data not shown). Moreover, immunohistochemical analysis did not reveal any differential expression of COX1, COX2, or EP4 receptors in DRG neurons of different sizes on the ipsilateral side (data not shown). Thus, presently, the reason for the activation of I_h currents by cAMP only in ipsilateral Aβ neurons remains to be determined. A possible explanation may be that EP4 receptors, which activate G_s and G_i under the physiologic condition, may be decoupled from G_i in these neurons under the neuropathic condition and sensitized to PGE_2 (Yokoyama et al., 2013). However, verifying this hypothesis in acutely isolated DRG neurons is challenging and hence is the limitation of this study.

To summarize, we propose the following two alternative scenarios of neuropathic pain based on our results. The first possibility is that the hyperexcitability of ipsilateral nociceptive Aβ neurons is solely responsible for neuropathic pain because they are also thermosensitive through the TRPV2 channels (Caterina et al., 1999; Fang et al., 2005). However, Emery et al. (2011) previously reported that mice whose *HCN2* was selectively disrupted in a subset of small neurons became refractory to the neuropathic pain. Thus, the second possibility is that PGE_2-activated C, Aδ, and Aβ neurons are all involved in neuropathic pain and that the hyperactive Aβ neurons may underlie tactile allodynia by inducing central hypersensitivity (Sukhotinsky et al., 2004). In the latter case, ivabradine and CJ-023423 will alleviate neuropathic pain by inhibiting the activated HCN2 channels of all these neurons in a cooperative manner. These considerations thereby strongly suggest the usefulness of ivabradine and CJ-023423 for neuropathic pain. However, ivabradine is a nonselective HCN channel inhibitor, and thus exerts a negative chronotropic effect on the heart (Noh et al., 2014; Young et al., 2014). Therefore, the development of novel HCN2-specific inhibitors in the near future is warranted.

Acknowledgments

We are grateful to Reiko Sakai for secretarial assistance.

Authorship Contributions

Participated in research design: Tanaka, Kawamata, Yamada.

Conducted experiments: Zhang, Kashihara, Nakada, Ishida, Fuseya, Kenkichi Kiyosawa.

Performed data analysis: Zhang, Kashihara, Nakada, Tanaka, Ishida, Yamada.

Wrote or contributed to the writing of the manuscript: Zhang, Kashihara, Tanaka, Kawagishi, Yamada.

References

Baron R (2006) Mechanisms of disease: neuropathic pain—a clinical perspective. *Nat Clin Pract Neurol* **2**:95–106.

Biel M (2009) Cyclic nucleotide-regulated cation channels. *J Biol Chem* **284**: 9017–9021.

Biel M, Wahl-Schott C, Michalakis S, and Zong X (2009) Hyperpolarization-activated cation channels: from genes to function. *Physiol Rev* **89**:847–885.

Bucchi A, Tognati A, Milanesi R, Baruscotti M, and DiFrancesco D (2006) Properties of ivabradine-induced block of HCN1 and HCN4 pacemaker channels. *J Physiol* **572**:335–346.

Caterina MJ, Rosen TA, Tominaga M, Brake AJ, and Julius D (1999) A capsaicin-receptor homologue with a high threshold for noxious heat. *Nature* **398**:436–441.

Chaplan SR, Bach FW, Pogrel JW, Chung JM, and Yaksh TL (1994) Quantitative assessment of tactile allodynia in the rat paw. *J Neurosci Methods* **53**:55–63.

Cohen SP and Mao J (2014) Neuropathic pain: mechanisms and their clinical implications [published correction appears in *BMJ* (2014) 348:g2323]. *BMJ* **348**: f7656.

Descoeur J, Pereira V, Pizzoccaro A, Francois A, Ling B, Maffre V, Couette B, Busserolles J, Courteix C, Noel J, et al. (2011) Oxaliplatin-induced cold hypersensitivity is due to remodelling of ion channel expression in nociceptors. *EMBO Mol Med* **3**:266–278.

Ebersberger A, Natura G, Eitner A, Halbhuber KJ, Rost R, and Schaible HG (2011) Effects of prostaglandin D2 on tetrodotoxin-resistant Na^+ currents in DRG neurons of adult rat. *Pain* **152**:1114–1126.

Emery AC, Eiden MV, and Eiden LE (2013) A new site and mechanism of action for the widely used adenylate cyclase inhibitor SQ22,536. *Mol Pharmacol* **83**:95–105.

Emery EC, Young GT, Berrocoso EM, Chen L, and McNaughton PA (2011) HCN2 ion channels play a central role in inflammatory and neuropathic pain. *Science* **333**: 1462–1466.

Emery EC, Young GT, and McNaughton PA (2012) HCN2 ion channels: an emerging role as the pacemakers of pain. *Trends Pharmacol Sci* **33**:456–463.

Fang X, McMullan S, Lawson SN, and Djouhri L (2005) Electrophysiological differences between nociceptive and non-nociceptive dorsal root ganglion neurones in the rat in vivo. *J Physiol* **565**:927–943.

Foehring RC and Waters RS (1991) Contributions of low-threshold calcium current and anomalous rectifier (I_h) to slow depolarizations underlying burst firing in human neocortical neurons in vitro. *Neurosci Lett* **124**:17–21.

Godínez-Chaparro B, López-Santillán FJ, Orduña P, and Granados-Soto V (2012) Secondary mechanical allodynia and hyperalgesia depend on descending facilitation mediated by spinal 5-HT_4, 5-HT_6 and 5-HT_7 receptors. *Neuroscience* **222**: 379–391.

Harper AA and Lawson SN (1985) Conduction velocity is related to morphological cell type in rat dorsal root ganglion neurones. *J Physiol* **359**:31–46.

Jaggi AS, Jain V, and Singh N (2011) Animal models of neuropathic pain. *Fundam Clin Pharmacol* **25**:1–28.
Jensen TS, Baron R, Haanpää M, Kalso E, Loeser JD, Rice AS, and Treede RD (2011) A new definition of neuropathic pain. *Pain* **152**:2204–2205.
Jones RL, Giembycz MA, and Woodward DF (2009) Prostanoid receptor antagonists: development strategies and therapeutic applications. *Br J Pharmacol* **158**: 104–145.
Jongsma H, Danielsen N, Sundler F, and Kanje M (2000) Alteration of PACAP distribution and PACAP receptor binding in the rat sensory nervous system following sciatic nerve transection. *Brain Res* **853**:186–196.
Kashihara T, Nakada T, Kojima K, Takeshita T, and Yamada M (2017) Angiotensin II activates Ca_V 1.2 Ca^{2+} channels through β-arrestin2 and casein kinase 2 in mouse immature cardiomyocytes. *J Physiol* **595**:4207–4225.
Kim KS, Kim J, Back SK, Im JY, Na HS, and Han PL (2007) Markedly attenuated acute and chronic pain responses in mice lacking adenylyl cyclase-5. *Genes Brain Behav* **6**:120–127.
Kouranova EV, Strassle BW, Ring RH, Bowlby MR, and Vasilyev DV (2008) Hyperpolarization-activated cyclic nucleotide-gated channel mRNA and protein expression in large versus small diameter dorsal root ganglion neurons: correlation with hyperpolarization-activated current gating. *Neuroscience* **153**:1008–1019.
Krames ES (2014) The role of the dorsal root ganglion in the development of neuropathic pain. *Pain Med* **15**:1669–1685.
Krames ES (2015) The dorsal root ganglion in chronic pain and as a target for neuromodulation: a review. Neuromodulation 18:24–32; discussion 32.
LaBuda CJ and Little PJ (2005) Pharmacological evaluation of the selective spinal nerve ligation model of neuropathic pain in the rat. *J Neurosci Methods* **144**: 175–181.
Lee CH and MacKinnon R (2017) Structures of the human HCN1 hyperpolarization-activated channel. *Cell* **168**:111–120.e11.
Ma W and St-Jacques B (2018) Signalling transduction events involved in agonist-induced PGE2/EP4 receptor externalization in cultured rat dorsal root ganglion neurons. *Eur J Pain* **22**:845–861.
Mabuchi T, Kojima H, Abe T, Takagi K, Sakurai M, Ohmiya Y, Uematsu S, Akira S, Watanabe K, and Ito S (2004) Membrane-associated prostaglandin E synthase-1 is required for neuropathic pain. *Neuroreport* **15**:1395–1398.
Momin A, Cadiou H, Mason A, and McNaughton PA (2008) Role of the hyperpolarization-activated current I_h in somatosensory neurons. *J Physiol* **586**: 5911–5929.
Moriyama T, Higashi T, Togashi K, Iida T, Segi E, Sugimoto Y, Tominaga T, Narumiya S, and Tominaga M (2005) Sensitization of TRPV1 by EP1 and IP reveals peripheral nociceptive mechanism of prostaglandins. *Mol Pain* **1**:3.
Noh S, Kumar N, Bukhanova N, Chen Y, Stemkowsi PL, and Smith PA (2014) The heart-rate-reducing agent, ivabradine, reduces mechanical allodynia in a rodent model of neuropathic pain. *Eur J Pain* **18**:1139–1147.
Ossovskaya VS and Bunnett NW (2004) Protease-activated receptors: contribution to physiology and disease. *Physiol Rev* **84**:579–621.
Scroggs RS, Todorovic SM, Anderson EG, and Fox AP (1994) Variation in IH, IIR, and ILEAK between acutely isolated adult rat dorsal root ganglion neurons of different size. *J Neurophysiol* **71**:271–279.
Segond von Banchet G, Pastor A, Biskup C, Schlegel C, Benndorf K, and Schaible HG (2002) Localization of functional calcitonin gene-related peptide binding sites in a subpopulation of cultured dorsal root ganglion neurons. *Neuroscience* **110**:131–145.
Sukhotinsky I, Ben-Dor E, Raber P, and Devor M (2004) Key role of the dorsal root ganglion in neuropathic tactile hypersensibility. *Eur J Pain* **8**:135–143.
van Hecke O, Austin SK, Khan RA, Smith BH, and Torrance N (2014) Neuropathic pain in the general population: a systematic review of epidemiological studies. *Pain* **155**:654–662.
Wainger BJ, DeGennaro M, Santoro B, Siegelbaum SA, and Tibbs GR (2001) Molecular mechanism of cAMP modulation of HCN pacemaker channels. *Nature* **411**: 805–810.
Wickenden AD, Maher MP, and Chaplan SR (2009) HCN pacemaker channels and pain: a drug discovery perspective. *Curr Pharm Des* **15**:2149–2168.
Yaksh TL and Rudy TA (1976) Chronic catheterization of the spinal subarachnoid space. *Physiol Behav* **17**:1031–1036.
Yokoyama U, Iwatsubo K, Umemura M, Fujita T, and Ishikawa Y (2013) The prostanoid EP4 receptor and its signaling pathway. *Pharmacol Rev* **65**:1010–1052.
Young GT, Emery EC, Mooney ER, Tsantoulas C, and McNaughton PA (2014) Inflammatory and neuropathic pain are rapidly suppressed by peripheral block of hyperpolarisation-activated cyclic nucleotide-gated ion channels. *Pain* **155**: 1708–1719.

Address correspondence to: Dr. Mitsuhiko Yamada, Department of Molecular Pharmacology, Shinshu University School of Medicine, 3-1-1 Asahi, Matsumoto, Nagano 390-8621, Japan. E-mail: myamada@shinshu-u.ac.jp